Available online at www.sciencedirect.com
SCIENCE DIRECT®
Journal of Molecular Graphics and Modelling 22 (2003) 105–114
Journal of Molecular Graphics and Modelling
www.elsevier.com/locate/JMGM

Computer-aided design of a factor Xa inhibitor by using MCSS functionality maps and a CAVEAT linker search

Yasunobu Takano [a,c,*], Masahiro Koizumi [a], Reiko Takarada [a], Midori Takimoto Kamimura [a], Ryszard Czerminski [b], Tohru Koike [c]

[a] *Medicinal Chemistry Research Department, Institute for Bio-Medical Research, Teijin Limited, 4-3-2 Asahigaoka, Hino, Tokyo 191-8512, Japan*
[b] *ArQule Inc., 19 Presidential Way, Woburn, MA 01801, USA*
[c] *Division of Medicinal Chemistry, Graduate School of Biomedical Sciences, Hiroshima University, Kasumi 1-2-3, Minami-ku, Hiroshima 734-8551, Japan*

Received 17 January 2003; received in revised form 12 April 2003; accepted 25 April 2003

Abstract

We have investigated a new approach to efficiently find a novel inhibitor against a serine protease (i.e. an activated coagulation factor X, FXa) by using de novo design programs and the X-ray crystal structure of the target enzyme. FXa is a coagulant enzyme that generates thrombin (a serine protease) and participates in both intrinsic and extrinsic coagulation pathways. We adopted multiple copy simultaneous search (MCSS) and CAVEAT linker search techniques, which disclosed a novel FXa inhibitor (T01312) consisting of two binding moieties (the benzamidinyl and adamantyl groups) and a linker unit (the carboxybenzylamine group). The inhibitory activity of T01312 against FXa was determined to be a small K_i-value of 48 nM, which is two orders of magnitude smaller than that against thrombin. An X-ray crystal analysis of T01312 complexed with trypsin (an analogue of FXa) and docking studies of T01312 with trypsin and FXa showed that: (i) the benzamidinyl group is a predominant binding moiety in the anionic pocket (S1 site) with an asparatic acid residue; (ii) a hydrophobic pocket (S4 site) is the binding site of the adamantyl group; (iii) the carboxylate group of the linker contributes to the selectivity for FXa against thrombin. Thus, the combination of the knowledge of the X-ray crystal structure of the target molecule with MCSS and CAVEAT linker search techniques proved to be an effective hit-finding method that does not require the screening of huge compound libraries.

Keywords: Structure-based design; MCSS; CAVEAT; Docking; Molecular modeling; Factor Xa inhibitor

1. Introduction

Finding hit compounds is the essential first step in the process to discover new drugs. The conventional approach is first to establish the in vitro assay system and then perform screening of an in-house compound library; however, this is not always the most cost-effective strategy. “In silico” screening is frequently utilized in order to decrease the number of compounds required for real screening when the target molecular structure is available. However, this method still has problems, such as the accuracy of the docking mode, the scoring functions, and the diversity of the compounds needed for database search. We investigated how to find a new hit compound efficiently with the X-ray structure of a target using de novo design programs.

Thromboembolic disease is caused by improper functioning of the blood coagulation process. The activated coagulation factor X (FXa) belongs to a family of trypsin—like serine proteases. Being essential for both the intrinsic and extrinsic pathways of the coagulation process, FXa holds a central position in the coagulation cascade and converts prothrombin to thrombin. Orally active FXa inhibitors have emerged as attractive anticoagulants that might not cause the problem of excessive bleeding that is associated with the use of thrombin inhibitors. Indeed, previous studies have shown that inhibitors of FXa might have a reduced side effect of bleeding compared with inhibitors of thrombin [1]. Therefore, the discovery of orally active FXa inhibitors could lead to improved treatment of chronic thromboembolic disorders. A number of companies have been searching for such agents, and a number of FXa inhibitors have been reported [2]. FXa can be inhibited by simple inhibitors such as 3-amidinobenzylphenylether [3], diamidinobenzofuranylethane (DABE) [4], and **1** (DX-9065a, see Fig. 1) [5] as well as by macromolecular inhibitors such as a tick anticoagulant peptide (TAP) [6].

The X-ray structure of ligandless FXa was reported [7] and has remarkable similarity in overall three-dimensional (3D) structure to other serine proteases, especially trypsin.

* Corresponding author. Tel.: +81-827-24-6525; fax: +81-827-24-6525.
E-mail address: y.takano@teijin.co.jp (Y. Takano).

1093-3263/$ – see front matter
doi:10.1016/S1093-3263(03)00140-2

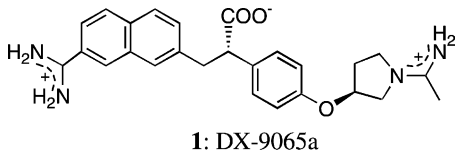

1: DX-9065a

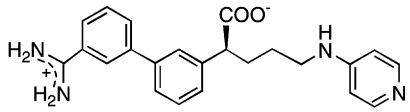

2: FX-2212a

Fig. 1. Chemical structures of FXa inhibitors, **1** and **2**, at physiological pH.

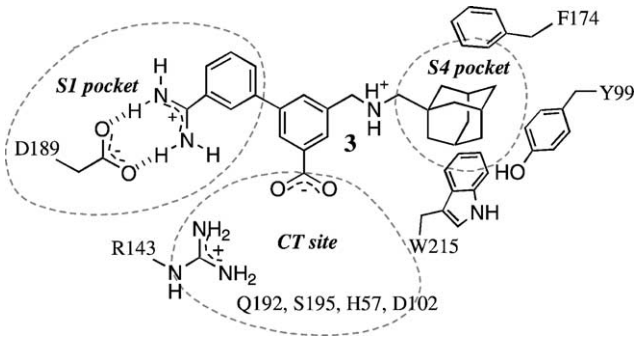

Fig. 2. A proposed binding mode of **3** in a FXa active site.

The co-crystal structures of FXa with small inhibitors, **1** and **2** (FX-2212a, see Fig. 1), have also been reported [8] and offer the prospect of structure-based drug design. These compounds have basic functional groups on both ends of the molecule. In the present paper, we report how to get a novel active compound utilizing the FXa crystal structure with de novo design programs.

2. Results and discussion

2.1. MCSS study on a novel FXa inhibitor

A multiple copy simultaneous search (MCSS) approach based on a local enhanced sampling (LES) method proposed by Elber and Karplus [9a] has been introduced for drug design as a pocket mapping methodology by Miranker and Karplus [9b]. The LES method is a useful approximation for studying the molecular dynamics (MD) of a small ligand interacting with a large molecule (e.g. protein). The main idea is to replace multiple MD runs of the "ligand + protein" system with a single run of a "many-ligand-copies + protein" system. As the vast majority of non-bonded interactions are protein–protein interactions and because the small ligand only slightly perturbs the motion of the protein, it is possible to study the motion of many copies of the ligand that do not interact with each other but which interact with full potential with the protein (which feels the averaged force from all ligand copies). This saves a great deal of computer time and, at the same time, yields results which approximate the actual physical system well, i.e. a single ligand interacting with a single protein. In the MCSS case, when the protein is treated as a rigid body fixed in space, this approximation becomes exact, and we effectively "map" the protein surface for the best interaction sites with a ligand by optimizing the orientations and conformations of non-interacting copies of the ligand in the potential field of the protein. Although it is possible, in principle, to allow for protein mobility, results are then more difficult to interpret—in this study, we consider only the rigid protein structure. Several studies have been reported about inhibitor design with MCSS; for example, Caflisch et al. demonstrated that the results of MCSS mapping of side chain fragments of amino acids, and of the acetamide fragment that mimics the backbone, were consistent with the structure of a potent inhibitor [9c].

The active site of FXa comprises three main areas from the standpoint of drug design. The S1 pocket is a narrow cleft with planar hydrophobic walls and Asp189 at the bottom. A positively charged group is favored in this pocket to make a salt bridge with the side chain of the asparatic acid. The S4 pocket consists of three aromatic amino acids: Phe174, Trp215, and Tyr99. A hydrophobic group as well as a positively charged group that makes a cation–π interaction is favored in the S4 pocket. The catalytic triad site (CT site) is composed of the triad residues (i.e. Ser195, His57, and Asp102) and neighboring residues (i.e. Gln192 and Arg143). The side chains of Ser195, Gln192, and Arg143 are fully exposed in the solvent for easy access by an inhibitor. Our hit mining was initiated with an MCSS fragment mapping with basic, hydrophobic, and acidic fragments in the active site of the FXa structure. Targeted interaction sites with the key residue numbers are shown in Fig. 2 together with our final designed FXa inhibitor **3** (T01312).

2.1.1. An appropriate moiety for the anionic S1 pocket

There are a huge number of small fragments for MCSS calculation if we select from possible and/or existing compounds, such as ACD. Instead of searching such a number of fragments, our strategy is selecting fragments for MCSS as small as possible with following three concepts: (i) classify fragments into aliphatics and aromatics, and select representatives from both of them; (ii) select the smallest fragments; (iii) add a methyl group as a linking vector in the fragment for the CAVEAT linker search.

From this point of view, three structures have been considered as candidate binding fragments for the S1 pocket: a methyl ammonium cation as an aliphatic amine and *p*- and *m*-methylbenzamidinium cations as aromatic amines. From the results of the MCSS study, there was no specific cluster of the minima in the active site for methyl ammonium (56 minima in the energy range between −98.5 and −4.9 kcal/mol). The lowest 6 minima in the energy range between −98.5 and −93.0 kcal/mol clustered in two positions, one in the

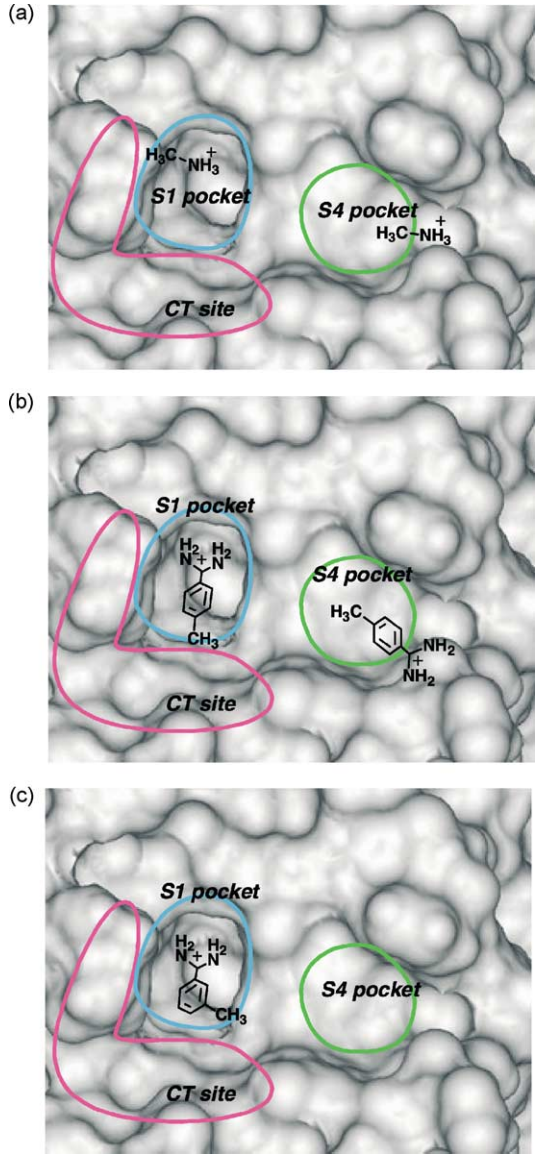

Fig. 3. Cluster positions of cations in a FXa active site: (a) methyl ammonium, (b) *p*-methylbenzamidinium, (c) *m*-methylbenzamidinium.

S1 pocket and the other in the S4 pocket interacting with the side chain of Glu97, which is located at the edge of the S4 pocket, as shown in Fig. 3a. Table 1 shows a summary of the MCSS results for methyl ammonium and the other fragments. In the case of *p*-methylbenzamidinium, the lowest 6 minima, whose energy range was between −80.4 and −64.0 kcal/mol, resulted in two clusters, as shown in Fig. 3b. One cluster was in the S1 pocket, making a salt bridge with Asp189, and the other, in the S4 pocket, interacting with Glu97. In the study with *m*-methylbenzamidinium, the lowest 6 minima consisted of only one cluster in the energy range from −78.9 to −60.0 kcal/mol, and all minima of this cluster were also making salt bridges with Asp189 in the S1 pocket, as shown in Fig. 3c. The methyl group of the lowest energy minimum of *m*-methylbenzamidinium was pointing into the S4 pocket. We selected this minimum as an S1 appropriate moiety for S1 pocket specificity and because of ease of linking to the S4 fragment.

2.1.2. An appropriate moiety for the hydrophobic S4 pocket

We recognized that it is very important for an inhibitor of FXa that each fragment interacts with the corresponding pockets effectively. So, our strategy is selecting the fragment whose cluster of the lowest minima locates in the middle of the S4 pocket to make an ideal interaction.

Three hydrophobic groups (tolyl, methylcyclohexyl, and 1-methyladamantyl) were utilized to map the S4 pocket. In the mapping study with the tolyl group, there was no specific cluster of the minima in the active site (142 minima in the energy range between −19.5 and −3.7 kcal/mol). The lowest 6 minima in the energy range between −19.5 and −18.0 kcal/mol clustered in only one position, as shown in Fig. 4a. A methylcyclohexyl group was used as a hydrophobic aliphatic group. The lowest 6 minima in the energy range between −16.8 and −15.6 kcal/mol clustered in only one position in the S1 pocket, as shown in Fig. 4b. In the third mapping study, an MCSS search with a more hindered 1-methyladamantyl group was performed. The lowest 6 minima in the energy range between −15.7 and −14.3 kcal/mol clustered in only one position in the S4 pocket, as shown in Fig. 4c. From these three MCSS mappings with hydrophobic fragments, the 1-methyladamantyl group was selected as an S4 fragment because only this group showed S4 pocket specificity. As in compounds **1** and **2**, basic groups may also be possible as S4 fragments for a cation–π interaction, but we think that a highly basic compound is not suitable as a hit compound for a further optimization stage for oral bioavailability reasons. Finally, the second-lowest energy minimum of 1-methyladamantyl MCSS mapping was selected as an appropriate moiety for the hydrophobic S4 pocket, since its methyl group was directed towards the S1 fragment and this geometric arrangement simplified connectivity.

Table 1
Summary of the MCSS results for various fragments in FXa

Fragments	No. of minima	No. of clusters	Lowest *E* (kcal/mol)	Highest *E* (kcal/mol)	Pocket
Methyl ammonium	6	2	−98.5	−93.0	S1, S4
p-Methylbenzamidinium	6	2	−80.4	−64.0	S1, S4
m-Methylbenzamidinium	6	1	−78.9	−60.0	S1
Toluene	6	1	−19.5	−18.0	Other
Methylcyclohexane	6	1	−16.8	−15.6	S1
1-Methyladamantane	6	1	−15.7	−14.3	S4

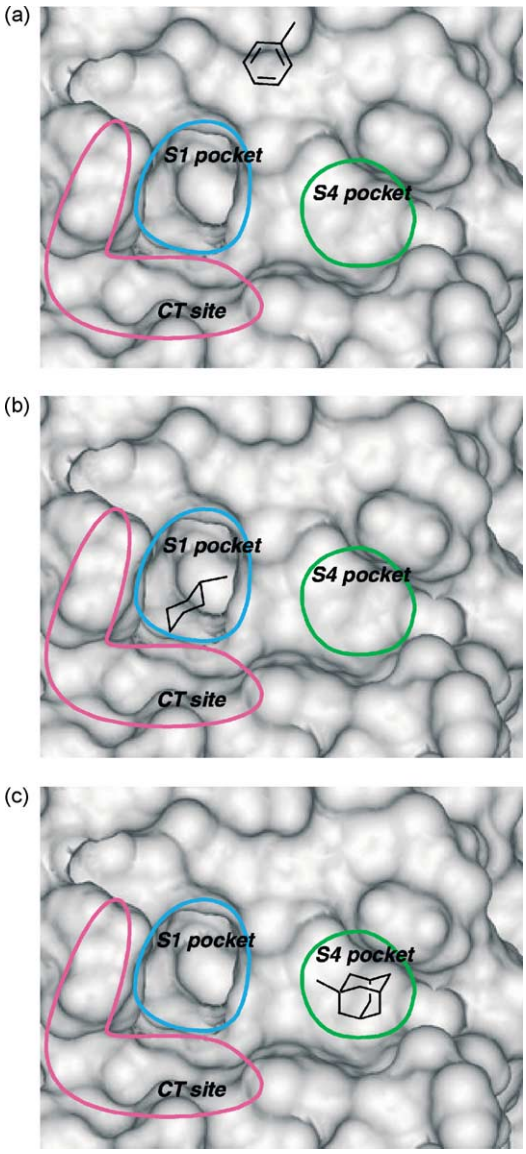

Fig. 4. Cluster positions of hydrophobic fragments in a FXa active site: (a) toluene, (b) methylcyclohexane, (c) 1-methyladamantane.

2.1.3. MCSS for a carboxylate binding site in FXa

In the acidic fragment mapping study, an acetate anion was selected as the minimum size of a fragment that possessed a linking methyl group. MCSS search resulted in 44 minima, which were classified into five clusters. The most densely populated cluster, which consisted of 14 minima, was located close to the CT site. The basicity of His57 was expected to be an important factor for this cluster. In the design of **1**, the acid group had been utilized for the selectivity from thrombin because of the repulsion of negative charges with thrombin [5a]. Our MCSS study suggests that adding an acid group as a CT site fragment to the molecule is also effective for getting a potent FXa inhibitor. As for this acetic acid residue, we did not select a specific minimum as a fragment in this stage because an ionic interaction does not need a vector-type interaction such as a hydrogen bond. This additional interaction was considered in the linker design stage (Fig. 5).

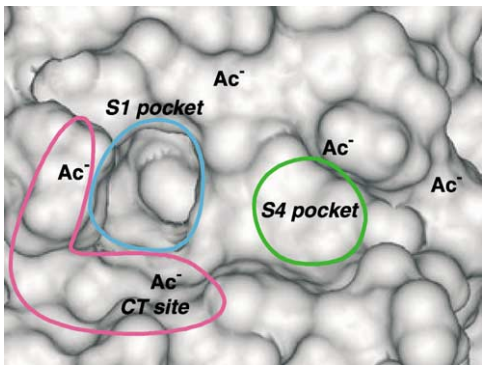

Fig. 5. Calculated binding positions for acetate anion (Ac^-) in a FXa active site.

2.2. CAVEAT linker search

Lauri and Bartlett proposed a linker search program, CAVEAT [10], as a method for organic molecular design. This program retrieves molecules from a 3D structural database with bonds that match a vector relationship defined by the query. CAVEAT is organized into three programs: VPREP, VSRCH, and CLASS. VPREP creates a CAVEAT database, which is essentially an index to the 3D structure source database. VSRCH searches this index for molecules that match the user's query. This search process is extremely fast because of the pre-computation in the VPREP step. CLASS processes the VSRCH results and classifies groups for user analysis. TRIAD and ILIAD databases for linker search are supplied with the CAVEAT program. TRIAD consists of minimized tricyclic hydrocarbons, and ILIAD contains more flexible acyclic structures.

Seven linker structures were retrieved by CAVEAT from the ILIAD database with two methyl groups of selected S1 and S4 minima given as the input vector queries. One of the linkers (Fig. 6a) has four bond lengths to connect both the amidinophenylmethyl group in the S1 pocket and the 1-methyladamantyl group in the S4 pocket, five linkers have five bonds (see Fig. 6b–f), and one linker has six bonds (see Fig. 6g). After a comparison of these seven linkers, the linker shown in Fig. 6b was selected for further study because of its natural biphenyl torsional angle and a carboxylate substitutable position on the linker phenyl ring.

Compound **3** was finally designed by connecting S1 and S4 fragments with the linker, removing the unnecessary exo-methyl group and changing sp^2 carbon to sp^3 carbon of the linker part, changing the carbon atom to a nitrogen atom in the linker because of the commercial availability of the starting material, and introducing a carboxylic group at the *meta* position of the linker phenyl group.

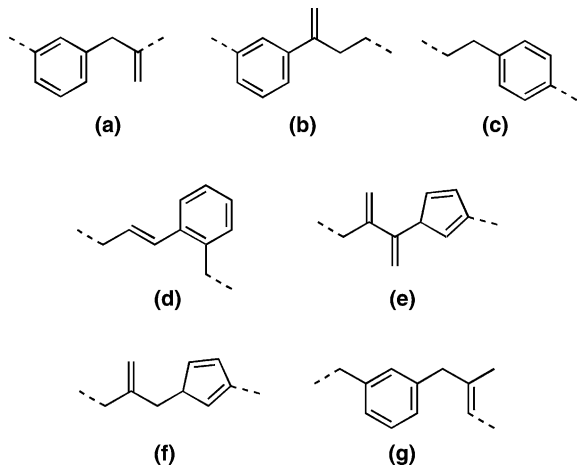

Fig. 6. Structures of the possible linker unit between *m*-benzyl and adamantyl groups.

2.3. Docking study of **3** and FXa

The structure **3** in FXa was minimized (see the white molecule in Fig. 7) using the molecular modeling program Quanta/CHARMm [11]. The original two minima selected, *m*-methylbenzamidinium and 1-methyladamantane (both in red), are shown in Fig. 7. The methylbenzamidinium group of **3** was located almost in the same position as the selected minima in the S1 pocket. The 1-methyladamantyl group of **3** was also in the same location as the selected minima in the S4 pocket. This result demonstrates that using the selected minima of the fragments and the modified linker is quite a reasonable approach to create a FXa inhibitor. Our experimental procedure to evaluate our inhibitor design strategy is described in Section 2.4.

2.4. Synthesis of **3**

The synthetic route of **3** is shown in Fig. 8. A starting compound, 3-methoxycarbonyl-5-nitrobenzoic acid **4**, was reduced with the borane–dimethylsulfide complex, and catalytic hydrogenation was then followed by iodination to obtain 3-hydroxymethyl-5-iodobenzoic acid methyl ester **5**. Suzuki coupling with 3-cyanobenzeneboronic acid in an aqueous solution afforded a biphenyl derivative **6**. After bromination of the hydroxyl group, an adamantyl derivative **7** was synthesized by reaction with adamantylmethylamine. Treatment with HCl in $MeOH/CH_2Cl_2$ followed by addition of NH_3 (i.e. the Pinner method) yielded a methyl ester **8** as its monohydrochloric acid salt. Hydrolysis of the methyl ester group in an aqueous solution gave the target compound **3** as a monohydrochloric acid salt in a total yield of 11%.

2.5. FXa inhibitory assay

The FXa inhibitory activities of the intermediate compound **8** and the final compound **3** were measured, and both of them were found to be a potent inhibitor ($K_i = 69$ and 48 nM, respectively), as expected. The compound **3** has high selectivity for FXa over thrombin ($K_i = 4.6\,\mu M$) and some selectivity over trypsin ($K_i = 70$ nM), whereas **8** has some selectivity for FXa over thrombin ($K_i = 250$ nM) and trypsin ($K_i = 190$ nM).

The carboxylate **3** was only slightly more potent than the ester **8** and we could not distinctly confirm the MCSS finding that the carboxylate favors the CT site. We suppose that the effect of the carboxylate might have been weakened by desolvation of the amino acids of the CT site, such as Arg143 and Ser195. The interaction of the carboxylate of **3** to trypsin and FXa did not significant effect to the inhibitory

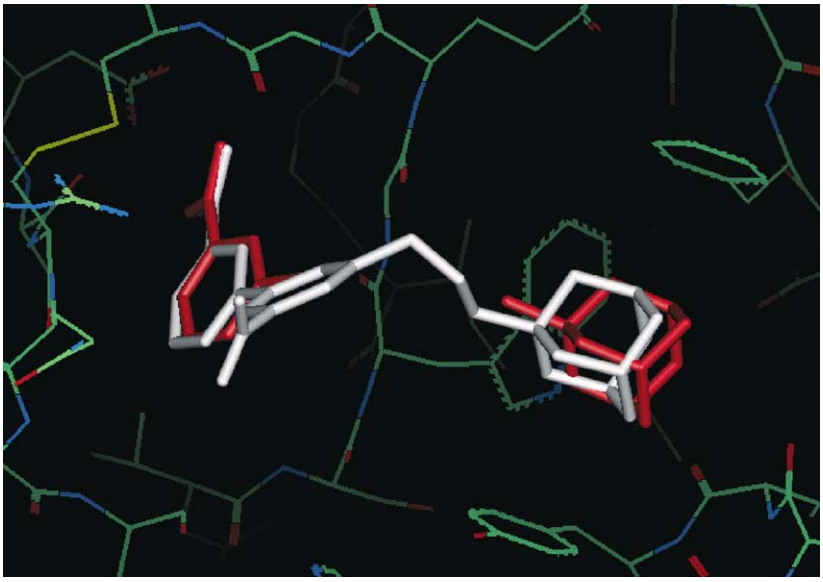

Fig. 7. Docking models of 1-methyladamantane (in red), *m*-methylbenzamidinium (in red), and **3** (in white) with FXa.

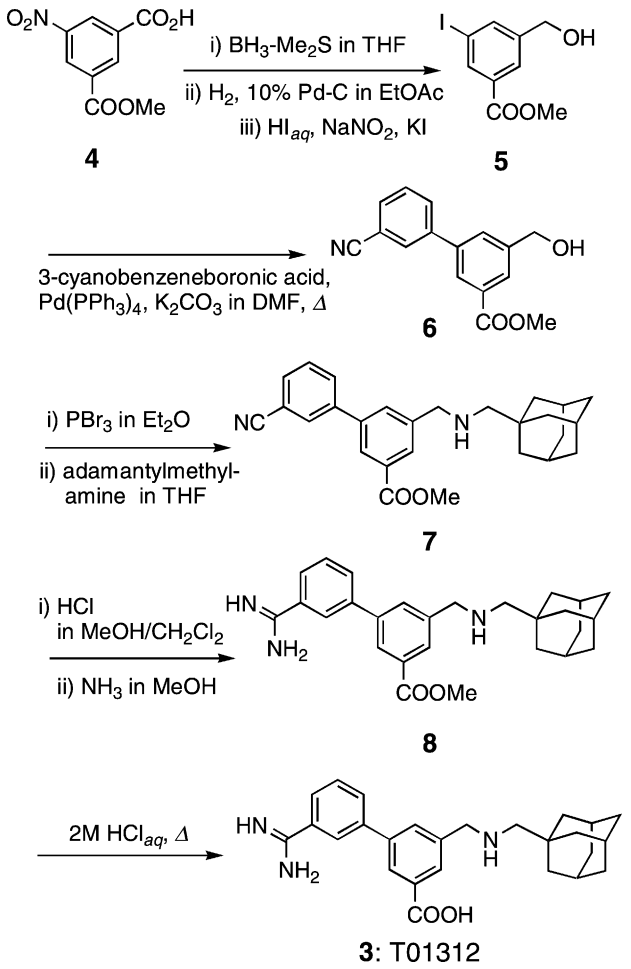

Fig. 8. Synthesis scheme for **3**.

activities even though the possibly interacting side chains of amino acids are different in both enzymes. On the other hand, the ionic repulsion between the carboxylic moiety of the inhibitor and the negatively charged amino acid group around the S1 pocket of thrombin seemed to increase the selectivity of **3** for FXa over thrombin, which was in accordance with the DX-9065a **1** study [5a].

The compound **3** inhibited the coagulation of human plasma in vitro, doubling the activated thromboplastin time (APTT) at a concentration of 2.2 μM. This shows that **3** is an effective inhibitor of FXa in the physiologically relevant human prothrombinase complex. We concluded that **3** was acceptable as a lead compound to develop chemistry for further optimization studies.

*2.6. An X-ray crystal analysis of trypsin-bound **3***

Since an appropriate co-crystal of **3** and FXa was not obtained for X-ray analysis, we determined an analogous co-crystal of **3** and bovine pancreatic trypsin (BPT), which was prepared in the presence of ammonium sulfate. Because of the similarity of trypsin to FXa, trypsin was sometimes utilized as a surrogate for FXa to determine the binding orientation and conformation of FXa inhibitors [2]. Fig. 9 shows the X-ray crystal structure of the co-crystal.

In the **3**-bound BPT complex, a sulfate anion was located close to the side chain of Ser195 and the ammonium group in the linker of **3**. Because of the strong negative charge, the hydroxyl and ammonium groups created hydrogen bonds with the sulfate. This strong interaction was expected to keep the carboxylate away from the CT site, and the adamantyl group pulled out from the S4 pocket. Even though the benzamidinyl

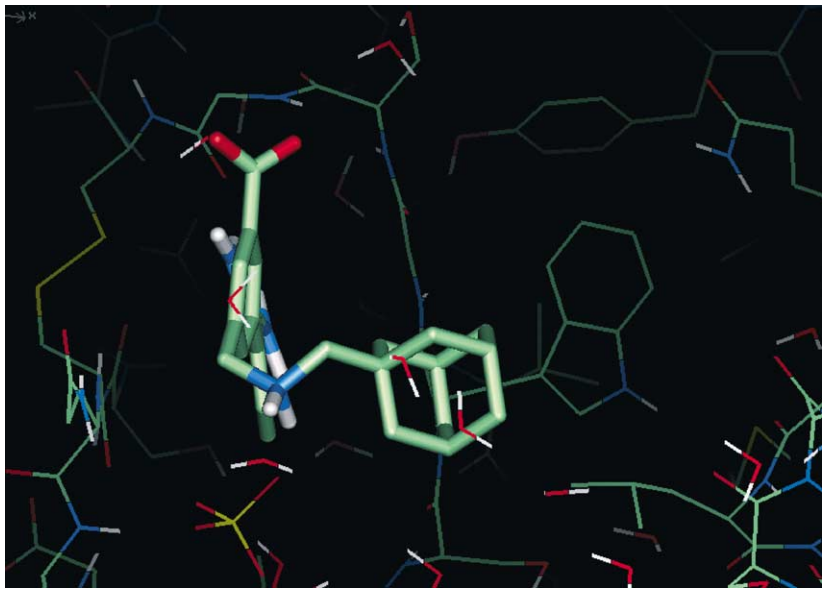

Fig. 9. X-ray crystal structure of **3** and bovine pancreatic trypsin.

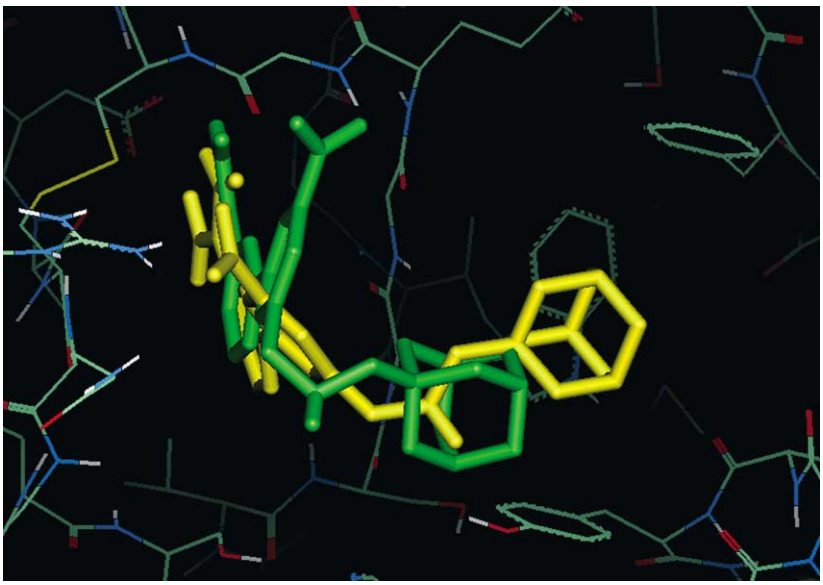

Fig. 10. Docking models with FXa: initial structure (in green) obtained from X-ray crystal analysis of **3**-bound BPT and minimized structure (in yellow).

group was in the same position in the S1 pocket, this binding orientation was different from our expectations based on the **3**-bound FXa model from the MCSS study.

Since sulfate anion is not present to a significant extent in ordinary biological systems, we conducted a modeling study with the X-ray structure of **3** in BPT as follows: (i) superimposition of the **3**-bound BPT and FXa, removal of BPT, the sulfate anion, and water molecules from the binding site, and (ii) minimization of the **3**-bound FXa structure (see the yellow structure in Fig. 10). The adamantyl and benzamidinyl groups in the calculated **3**-bound FXa were almost in the same positions as we had previously modeled "in silico". The positions and orientations of the fragments of **3**, which derived from the hydrogen bond, the ionic interaction, and the hydrophobic interaction, are consistent with the high potent activity as a FXa inhibitor.

3. Conclusions

We have found a novel potent FXa inhibitor **3** (T01312) by combination of the MCSS fragment mapping technique and the CAVEAT linker search method. The inhibitory activity of **3** against FXa was determined to be a K_i-value of 48 nM, which is two orders of magnitude smaller than that against thrombin. Furthermore, the modeling study with **3**-bound bovine pancreatic trypsin co-crystal data supports the positions and orientations obtained from the initial MCSS mapping. Thus, we demonstrated that the combination of MCSS and CAVEAT linker search techniques is an effective strategy for a novel hit finding that can be used as an alternative method to large scale screening. This potent lead compound **3** has been selected for further FXa inhibitor investigation in our laboratory.

4. Materials and methods

4.1. Computational methods

All calculations were performed using a SGI OCTANE workstation with two R10000 processors. Molecular graphics operations were accomplished using Quanta, version 2000, and InsightII, version 2000 [11]. MCSS, energy calculations, and minimization were performed using the commercial version of Accelrys CHARMm and the academic version of CHARMM23.2 [11]. The CAVEAT, version 2.2 [10a] was used for linker search.

To prepare the FXa structure for use with MCSS calculation, hydrogens were added in InsightII (at pH 7.0) to the human FXa X-ray structure reported by Padmanabhan et al. [7] (PDB accession number 1HCG), and water molecules were removed. The active site was defined as a sphere with its center at the N of Gly217 and a radius of 12 Å. All functional groups for MCSS were constructed with InsightII. Partial charges were calculated with cff. Ten iterations of the following procedure were performed. The site was filled with 100 copies of each functional group with random positions and orientations and minimized using the steepest-descent algorithm. The minimum distance allowed to the protein per group in the initial random distribution was 1.2 Å, and the non-bond cutoff distance was 7.5 Å. The energy tolerance for group in the initial distribution was 500 and 0 kcal/mol after the minimization. Functional groups that converged to the same minima were eliminated based on an RMS cutoff of 0.2 Å. Only minima with negative energies were further investigated.

For minima identified in the MCSS calculation, a CAVEAT linker search was performed. CAVEAT finds structures that satisfy the required geometrical relationship

between specified bonds by screening large databases. The two methyl groups of selected S1 and S4 minima were used as the input vector queries. The distance tolerance was 0.05 Å and the angle tolerance was 0.05 rad. The ILIAD database was selected for the linker search. The hit compounds are classified into a structural subgraph, and the necessary motifs are identified [10a]. All linker structures were imported to Quanta for the modeling study.

A designed molecule was minimized in the field of FXa. During minimization, the ligand was not constrained; all FXa atoms within 7 Å of the ligand were constrained with 10 kcal/mol harmonic constraints, and all FXa atoms between 7 and 14 Å from the ligand were constrained with 25 kcal/mol harmonic constraints. The coordinates of all FXa atoms further than 14 Å from the ligand were fixed. Minimization, using a conjugate gradient algorithm, was continued until the energy gradient was smaller than 0.01 kcal/mol.

4.2. Synthetic method

All starting materials, reagents, and solvents were used as acquired from commercial sources without purification. In general, reactions were performed under a dry nitrogen atmosphere unless noted. Medium-pressure liquid chromatography (MPLC) was carried out on Daisogel IR-60 silica gel. Generally, final products were purified with preparative HPLC, which was performed using a reverse-phase ODS column (Nacalai Tesque, Cosmosil 5C18-AR, 20 × 250 mm), a mobile phase of MeOH–water (5/95–95/5) containing 0.1% TFA, and a flow rate of 10 ml/min. Fractions containing the desired material were concentrated and lyophilized.

^{1}H NMR spectra were recorded on JEOL EX-270 FT-NMR at 270 MHz and JEOL JNM-ECP 500 at 500 MHz, and ^{13}C NMR spectra were recorded at 125 MHz. Data measured by JEOL JNM-ECP 500 are marked with an asterisk. The chemical shifts are given in ppm (δ) from tetramethylsilane, which was used as an internal standard. Mass spectra were obtained from a PE-SCIEX API100 LC–MS system with the electrospray ionization method (ESI). Elemental analyses were performed using Perkin-Elmer 2400 Series II CHN/O analyzer.

4.2.1. Methyl 3-hydroxymethyl-5-iodobenzoate (**5**)

To a stirred solution of 3-nitro-5-methoxycarbonylbenzoic acid (85 g, 0.378 mol) in THF (200 ml), the borane–dimethylsulfide complex (43.4 ml, 0.458 mol) was added at 0 °C and then stirred for 18 h. To the solution, water (200 ml) was added, followed by K_2CO_3 (96 g, 0.694 mol), and extracted by EtOAc (2 × 150 ml). The combined organic extracts were washed with brine, dried on $MgSO_4$, and concentrated in vacuo. The residue was dissolved in EtOAc (800 ml), and 10% Pd/C (750 mg) was then added and hydrogenated under a hydrogen atmosphere. After hydrogenation was finished, the reaction mixture was filtered through a pad of celite, and the filtrate was concentrated to afford crude methyl 3-amino-5-hydroxy-methylbenzoate (64 g, 0.353 mol). ^{1}H NMR ($CDCl_3$): δ 7.39 (s, 1H), 7.26 (s, 1H), 6.89 (s, 1H), 4.64 (s, 1H), 3.89 (s, 3H), 2.30 (s, 1H).

To a solution of crude methyl 3-amino-5-hydroxymethylbenzoate (34.3 g) in THF (200 ml), hydroiodic acid (75 g) was added at 0 °C and then stirred for 5 min. To this stirred solution, sodium nitrite solution (13.7 g of sodium nitrite dissolved in 100 ml of water) was added from −5 to 5 °C and then stirred for 40 min at 0 °C. To this diazonium solution, a potassium iodide solution (34.6 g of potassium iodide was dissolved in 150 ml of water) was added and then stirred for 2 h at 40 °C. Water (300 ml) was added, concentrated in vacuo, and extracted by EtOAc (3 × 150 ml). The combined organic extracts were washed with brine, dried with $MgSO_4$, and concentrated in vacuo, and the residue was chromatographed over silica gel with a gradient of *n*-hexane/EtOAc to yield **5** as a colorless oil (23.1 g, 79.1 mmol, 41.8%). ^{1}H NMR ($CDCl_3$): δ 8.29 (s, 1H), 7.98 (s, 1H), 7.93 (s, 1H), 4.72 (d, J = 5.6 Hz, 1H), 3.92 (s, 3H), 1.81 (t, J = 5.6 Hz, 1H).

4.2.2. Methyl 3-(3-cyanophenyl)-5-hydroxymethylbenzoate (**6**)

To a stirred solution of compound **5** (3.08 g, 10.5 mmol) in DMF (50 ml), (3-cyanophenyl)boronic acid (2.32 g, 15.8 mmol), K_2CO_3 (2.18 g, 15.8 mmol), and tetrakis(triphenylphosphine)palladium(0) (456 mg, 0.366 mmol) were added. The reaction mixture was stirred at 90 °C overnight, and water (100 ml) was then added; the reaction mixture was extracted with EtOAc (2 × 100 ml). The combined organic extracts were dried on $MgSO_4$ and then concentrated in vacuo.

The residue was purified by MPLC with a gradient of *n*-hexane/EtOAc/CH_2Cl_2 (1/1/1–2/3/1) to give **6** (2.05 g, 7.67 mmol, 73.0%) as a colorless solid. ^{1}H NMR ($CDCl_3$): δ 8.2–7.5 (m, 7H), 4.84 (d, J = 3.7 Hz, 2H), 3.96 (s, 3H), 2.1 (br s, 1H).

4.2.3. Methyl 3-[(adamantanylmethyl)amino]methyl-5-(3-cyanophenyl)benzoate (**7**)

To a mixture of compound **6** (661 mg, 2.47 mmol) in Et_2O (20 ml), PBr_3 (117 ml, 1.24 mmol) was slowly added and stirred at room temperature for 19 h. The reaction mixture was diluted with Et_2O, washed with brine, dried on $MgSO_4$, and concentrated in vacuo. The residue was purified with silica gel chromatography (CH_2Cl_2) to afford methyl 3-(3-bromo-methyl)-5-cyanophenylbenzoate (719 mg, 2.18 mmol, 88.2%) as a light-yellow solid. ^{1}H NMR ($CDCl_3$): δ 8.2–8.1 (m, 2H), 7.9–7.5 (m, 5H), 4.58 (s, 2H), 3.96 (s, 3H). This bromide (300 mg, 0.909 mmol) was dissolved in THF (5.0 ml), and 1-adamantanemethylamine (322 mg, 1.82 mmol) was added. This solution was stirred overnight at room temperature.

The solution was concentrated in vacuo, and the residue was purified by MPLC with a gradient of *n*-hexane/EtOAc (4/1–7/3) to give **7** (320 mg, 0.772 mmol, 84.9%) as a

colorless solid. ^{1}H NMR ($CDCl_3$): δ 8.12 (s, 1H), 8.03 (s, 1H), 8.0–7.8 (m, 3H), 7.77 (s, 1H), 7.64 (d, J = 7.5 Hz, 1H), 7.57 (t, J = 7.5 Hz, 1H), 3.96 (s, 3H), 3.90 (s, 2H), 2.27 (s, 2H), 1.97 (s, 3H), 1.8–1.6 (m, 6H), 1.54 (s, 6H).

4.2.4. Methyl 3-[(adamantanylmethyl)amino]methyl-5-(3-amidinophenyl)benzoate (**8**)

A solution of **7** (320 mg, 0.772 mmol) in CH_2Cl_2 (25 ml) and MeOH (1.0 ml) was saturated with HCl gas with ice cooling by bubbling for 30 min, and then the reaction vessel was sealed and allowed to stand for 16 h at room temperature. Then, the solvents were removed in vacuo, and the resulting residue was dissolved in 10 ml of a methanolic ammonia solution (previously, ammonia gas was bubbled through the MeOH for 30 min with ice cooling) and stirred for 6 h at room temperature. After removal of the solvent, the resulting residue was purified by preparative HPLC. After addition of a small amount of concentrated HCl, the selected fractions were concentrated and lyophilized to give **8** (265 mg, 0.478 mmol, 61.9%) as a colorless solid. ^{1}H NMR ($CDCl_3$): δ 8.74 (s, 1H), 8.39 (s, 1H), 8.1–7.9 (m, 3H), 7.75 (d, J = 8.0 Hz, 1H), 7.49 (t, J = 8.0 Hz, 1H), 4.30 (s, 2H), 3.88 (s, 3H), 2.59 (s, 2H), 1.91 (s, 3H), 1.64 (br s, 6H), 1.58 (br s, 6H). MS (EI) *m/e* 432 $(MH)^+$. Analytically calculated for $C_{27}H_{33}N_3O_2{\cdot}HCl{\cdot}3H_2O$: C, 58.52; H, 7.28; N, 7.58. Found: C, 58.54; H, 7.41; N, 7.50.

4.2.5. 3-[(adamantanylmethyl)amino]methyl-5-(3-amidinophenyl)benzoic acid (**3**)

A solution of **8** (180 mg, 0.325 mmol) in 2 M HCl was heated at 80 °C for 24 h. After evaporation of the solvent, the residue was purified by preparative HPLC ($MeOH/H_2O/CH_3COOH$, 35/65/0.1). The selected fractions were lyophilized to give **3** (114 mg, 0.216 mmol, 66.5%) as a colorless solid. ^{1}H NMR (DMSO-d_6): δ 9.52 (br s, 2H), 9.33 (br s, 2H), 8.41 (dd, J = 1.6, 1.6 Hz, 1H), 8.39 (dd, J = 1.6, 1.6 Hz, 1H), 8.21 (dd, J = 1.6, 1.6 Hz, 1H), 8.24 (dd, J = 1.8, 1.8 Hz, 1H), 8.13 (ddd, J = 7.8, 1.8, 0.9 Hz, 1H), 7.89 (ddd, J = 7.8, 1.8, 0.9 Hz, 1H), 7.77 (dd, J = 7.8, 7.8 Hz, 1H), 4.30 (s, 2H), 2.62 (s, 2H), 1.95 (br s, 3H), 1.67–1.59 (m, 12H). ^{13}C NMR (DMSO-d_6): δ 167.5, 166.1, 140.0, 139.8, 134.1, 133.9, 132.8, 132.5, 131.5, 130.4, 129.5, 128.4, 128.2, 127.2, 58.7, 51.5, 39.7, 36.5, 32.5, 28.0. MS (EI) *m/e* 418 $(MH)^+$. Analytically calculated for $C_{26}H_{31}N_3O_2{\cdot}HCl{\cdot}4H_2O$: C, 59.36; H, 7.67; N, 7.98. Found: C, 59.09; H, 7.39; N, 8.15.

4.3. Enzyme and coagulation assay

Human FXa (Enzyme Research Laboratories Inc.), human thrombin (Sigma), and human pancreatic trypsin (Athens Research International Inc.) were used from commercial sources. The chromogenic substrates used were S-2765 for FXa; S-2238 for thrombin; and S-2444 for trypsin, and each was purchased from Chromogenix. FXa was assayed in a buffer containing 50 mM Tris, 0.15 M NaCl, 5.0 mM $CaCl_2$, 0.1% (w/v) PEG 8000, and 0.11% BSA at pH 8.3. Trypsin was assayed in a buffer containing 50 mM Tris, 0.11 M NaCl, and 0.1% (w/v) PEG 8000 at pH 8.0. Thrombin was assayed in a buffer containing 50 mM Tris, 0.15 M NaCl, and 0.1% (w/v) PEG 8000 at pH 8.4. The final substrate concentrations in the reactions were 100, 200, and 400 μM for FXa and 50, 100, and 200 μM for trypsin. These two assays were run in 96-well microtiter plates, and the hydrolysis rates were determined at 405 nm using a Thermomax plate reader (Molecular Devices). For the thrombin inhibitory assay, the final substrate concentrations were 2.5, 3.75, 5.0, 7.5, and 10 μM, and the enzyme reaction was performed in a cuvette. The hydrolysis rates were determined at 405 nm using a UV-2100 spectrometer (Shimazu Co.). K_i-values were calculated according to the Lineweaver–Burk method.

Activated partial thromboplastin time (APTT) was measured with Amelung Coagulometer KC-10A. Plasma (100 μl) and a solution of an inhibitor were mixed with 100 μl of an actin-activated cephaloplastin reagent (Dade Behring Inc.), and the coagulation was started with 100 μl of 25 mM $CaCl_2$.

4.4. X-ray crystallography

β-Trypsin was purchased from Sigma (bovine pancreatic trypsin, T-8642). The compound **3** was added to the trypsin solution, 30 mg/ml in 50 mM Tris–HCl (pH 7.5), with a molar ratio of 10:1 for co-crystallization. The complex crystals were grown from 24% (w/v) polyethylene glycol (PEG) 8000, 0.1 M Tris–HCl (pH 7.5), 0.20 M ammonium sulfate, 5.0 mM $CaCl_2$, and 2% (v/v) DMSO using the sitting-drop vapor diffusion method.

The crystal was mounted in a glass capillary and exposed to X-ray radiation at room temperature on a rotating anode generator (RU-H3RHF, Rigaku Corporation) equipped with an Raxis-IIc imaging plate detector. The obtained crystals belong to the space group $P3_121$ with unit cell constants $a = b = 55.1$ Å and $c = 109.4$ Å and have one molecular complex per asymmetric unit. The X-ray data were processed and scaled using PROCESS [12] and comprised 14721 unique reflections with $|F| > 2\sigma(F)$ derived from 67427 intensity measurements, with an R_{merge} of 5.92% and a completeness of 95.4%.

The complex structure was solved by molecular replacement using the coordinates of trypsin (PDB accession number 1TLD [13]) as the search model. Calculations were done using X-PLOR, version 3.1 [14]. Very clear solutions were found for both rotation and translation functions. Rigid body refinement reduced the R-factor from 0.359 to 0.285 in the resolution range from 10 to 4.0 Å. The protein structure was refined alternatively with X-PLOR and ProLSQ95 [11], and the model was improved on the basis of $|F_o - F_c|$ and $|2F_o - F_c|$ maps with Quanta. The position of **3** near the active site was clearly identified using X-LIGAND [11]. The final model contained one trypsin molecule, one sulfate ion, 107 water molecules, and one inhibitor molecule. The final

R-factor (defined as $R = \Sigma||F_o| - |F_c||/\Sigma|F_o|$) was 0.135 in the resolution range from 5.0 to 1.9 Å for 11090 reflections with F_o greater than 2σ.

Acknowledgements

The authors gratefully acknowledge helpful discussions with Dr. Peter Gund (Accelrys Inc.). Y. Takano would like to thank Dr. Kazuhiro Ohtani (Hiroshima University) for valuable advice on the NMR analysis. Y. Takano also wishes to thank Tomohisa Nakada, Takayuki Hara, Satoshi Sugiura, and Yoshiharu Takazawa (Teijin Ltd.) for valuable discussions.

References

[1] Y. Morishima, K. Tanabe, Y. Terada, T. Hara, S. Kunitada, Antithrombotic and hemorrhagic effects of DX-9065a, a direct and selective factor Xa inhibitor: comparison with a direct thrombin inhibitor and antithrombin III-dependent anticoagulants, Thromb. Haemost. 78 (1997) 1366–1371.

[2] (a) D.J. Pinto, M.J. Orwat, S. Wang, J.M. Fevig, M.L. Quan, E. Amparo, J. Cacciola, K.A. Rossi, R.S. Alexander, A.M. Smallwood, J.M. Luettgen, L. Liang, B.J. Aungst, M.R. Wright, R.M. Knabb, P.C. Wong, R.R. Wexler, P.Y.S. Lam, Discovery of 1-[3-(aminomethyl)phenyl]-*N*-[3-fluoro-2′-(methylsulfonyl)-[1,1′-biphenyl]-4-yl]-3-(trifluoromethyl)-1H-pyrazole-5-carboxamide (DPC423), a highly potent, selective, and orally bioavailable inhibitor of blood coagulation factor Xa, J. Med. Chem. 44 (2001) 566–578;
(b) M.L. Quan, R.R. Wexler, The design and synthesis of non-covalent factor Xa inhibitors, Curr. Top. Med. Chem. 1 (2001) 137–149.

[3] J. Hauptmann, F. Markwardt, P. Walsmann, Synthetic inhibitors of serine proteinases. Part XVI: Influence of 3- and 4-amidinobenzyl derivatives on the formation and activation of thrombin, Thromb. Res. 12 (1978) 735–744.

[4] R.R. Tidwell, W.P. Webster, S.R. Shaver, J.D. Geratz, Strategies for anticoagulation with synthetic protease inhibitors: Xa inhibitors versus thrombin inhibitors, Thromb. Res. 19 (1980) 339–349.

[5] (a) T. Nagahara, Y. Yokoyama, K. Inamura, S. Katakura, S. Komoriya, H. Yamaguchi, T. Hara, M. Iwamoto, Dibasic (amidinoaryl)propanoic acid derivatives as novel blood coagulation factor Xa inhibitors, J. Med. Chem. 37 (1994) 1200–1207;
(b) S. Katakura, T. Nagahara, T. Hara, S. Kunitada, M. Iwamoto, Molecular model of an interaction between factor Xa and DX-9065a, a novel factor Xa inhibitor: contribution of the acetimidoylpyrrolidine moiety of the inhibitor to potency and selectivity for serine proteases, Eur. J. Med. Chem. 30 (1995) 387–394.

[6] L. Waxman, D.E. Smith, K.E. Arcuri, G.P. Vlasuk, Tick anticoagulant peptide (TAP) is a novel inhibitor of blood coagulation factor Xa, Science 248 (1990) 593–596.

[7] K. Padmanabhan, K.P. Padmanabhan, A. Tulinsky, C.H. Park, W. Bode, R. Huber, D.T. Blankenship, A.D. Cardin, W. Kisiel, Structure of human Des(1–45) factor Xa at 2.2 Å resolution, J. Mol. Biol. 232 (1993) 947–966.

[8] (a) H. Brandstetter, A. Kühne, W. Bode, R. Huber, W. Saal, K. Wirthensohn, R.A. Engh, X-ray structure of active site-inhibited clotting factor Xa, J. Biol. Chem. 271 (1996) 29988–29992;
(b) K. Kamata, H. Kawamoto, T. Honma, T. Iwama, S.H. Kim, Structural basis for chemical inhibition of human blood coagulation factor Xa, Proc. Natl. Acad. Sci. U.S.A. 95 (1998) 6630–6635.

[9] (a) R. Elber, M. Karplus, Enhanced sampling in molecular dynamics: use of the time-dependent Hartree approximation for a simulation of carbon monoxide diffusion through myoglobin, J. Am. Chem. Soc. 112 (1990) 9161–9175;
(b) A. Miranker, M. Karplus, Functionality maps of binding sites: a multiple copy simultaneous search method, Proteins 11 (1991) 29–34;
(c) A. Caflisch, A. Miranker, M. Karplus, Multiple copy simultaneous search and construction of ligands in binding sites: application to inhibitors of HIV-1 aspartic proteinase, J. Med. Chem. 36 (1993) 2142–2167.

[10] (a) G. Lauri, P.A. Bartlett, CAVEAT: a program to facilitate the design of organic molecules, J. Comput. Aided Mol. Des. 8 (1994) 51–66;
(b) D.R. Artis, C. Brotherton-Pleiss, J.H.B. Pease, C.J. Lin, S.W. Ferla, S.R. Newman, S. Bhakta, H. Ostrelich, K. Jarnagin, Structure-based design of six novel classes of non-peptide antagonists of the bradykinin B_2 receptor, Bioorg. Med. Chem. Lett. 10 (2000) 2421–2425.

[11] Accelrys Inc., San Diego, CA.

[12] PROCESS, R-AXIS data-processing software, Rigaku Corporation, 1996.

[13] H.D. Bartunik, L.J. Summers, H.H. Bartsch, Crystal structure of bovine β-trypsin at 1.5 Å resolution in a crystal form with low molecular packing density: active site geometry, ion pairs and solvent structure, J. Mol. Biol. 210 (1989) 813–828.

[14] (a) A.T. Brünger, Free *R*-value: a novel statistical quantity for assessing the accuracy of crystal structures, Nature 355 (1992) 472–475;
(b) A.T. Brünger, X-PLOR, version 3.1, A system for X-ray crystallography and NMR, Yale University Press, New Haven, CT, 1992.